EPR INVESTIGATION OF MANGANESE IONS IN $70TeO_2 \cdot 25B_2O_3 \cdot 5MO$ (MO $\Rightarrow$ SrO or SrF_2) GLASS MATRICES

I. Ardelean[*], M. Peteanu, N. Mureşan, V. Ioncu, F. Ciorcas-Delille[a]

Faculty of Physics, Babeş-Bolyai University, 400048 Cluj-Napoca, Romania
[a]C.E.A-D.R.F.M.C. SPINTEC, 38527 Grenoble, Cedex 9, France

EPR of Mn^{2+} ions revealed their distribution on different structural units in $70TeO_2 \cdot 25B_2O_3 \cdot 5MO$ (MO $\Rightarrow$ SrO or SrF_2) glass matrices. The number of isolated Mn^{2+} ions, participating at the $g_{eff} \approx 4.3$ resonance increase up to 1 mol % MnO and after that decreases to nil for 10 mol % MnO and was not affected by replacing of SrO with SrF_2. The number of Mn^{2+} ions participating at the $g_{eff} \approx 2.0$ resonance increases when the MnO content rises. In the case of the matrix with SrO the number of these ions are only a little higher than that of the matrix with SrF_2 for $5 \leq x \leq 30$ mol %, but for $x > 30$ mol % their content are higher in case of the matrix with SrF_2. From line-width composition dependence the effect of replacing of SrO with SrF_2 was to accentuate the clusterizing tendencies of manganese ions when increasing the MnO content, attested by a more pronounced narrowing of the line at $g_{eff} \approx 2.0$.

1. Introduction

Structural characteristics and properties of vitreous systems containing manganese may be revealed by means of EPR. Being very sensitive to changes in its neighbourhood the Mn^{2+} paramagnetic ion may provide valuable information about the structural units evolution, the type and strengths of bondings, the valence state, the involved interactions, etc. [1-6]. Various earlier investigations concern borate [7-12], boro-tellurite [13, 14], silicate [4, 15, 16], phosphate [16] oxide glasses, chalcogenide [17, 18] and halide [5, 6] glasses studied by means of Mn^{2+} ions absorption spectra, followed when the impurity ions content varies within a given concentration range. Generally, the spectra consist of resonance lines centered at $g_{eff} \approx 2.0$, 4.3 and 3.3 values. The $g_{eff} \approx 2.0$ may be attributed to isolated Mn^{2+} ions in octahedrally symmetric sites, slightly tetragonally distorted usually having a resolved hyperfine structure (hfs) or to associated ones, the Mn^{2+} ions being involved in dipole-dipole and/or superexchange interactions [19]. The strongly distorted versions of the octahedral vicinity of isolated Mn^{2+} ions subjected to strong field effects, given rise to absorbtions at $g_{eff} \approx 4.3$ and 3.3 [4, 5]. A special effort was made to elaborate the theoretical support for explaining the resonance lines at $g_{eff} \approx 4.3$ and 3.3 from the Mn^{2+} ions EPR spectra [1-7, 20, 21].

In an earlier paper [22] we investigated by EPR the system $xMnO \cdot [70TeO_2 \cdot 25B_2O_3 \cdot 5PbO]$.

In this paper we present two series of glasses, namely $xMnO \cdot (100-x)[70TeO_2 \cdot 25B_2O_3 \cdot 5SrO]$ and $xMnO \cdot (100-x)[70TeO_2 \cdot 25B_2O_3 \cdot 5SrF_2]$, which were prepared for $0.1 \leq x \leq 50$ mol % and studied by means of EPR.

---

[*] Corresponding author: arde@phys.ubbcluj.ro

2. Experimental

The starting materials used in the present investigation were $MnCO_3$, TeO_2, H_3BO_3, $SrCO_3$ or SrF_2 of reagent grade purity. The samples were prepared by weighing suitable proportions of the components powder mixing and mixture melting in sintered corundum crucibles at 1000 ^{o}C for 6 minutes. The mixtures were put into the electrical furnace directly at this temperature. The molten material was quenched by pouring it onto a copper plate held at room temperature. The X-ray patterns of the investigated samples are characteristic for vitreous systems. For these two series of samples no crystalline phase was observed up to x = 50 mol %.

The EPR measurements were recorded at room temperature in X-band (9.45 GHz) and 100 KHz field modulation with a Bruker ESR 300 E spectrometer. To avoid the alteration of the glass structure due to the ambient conditions, especially humidity, samples were poured immediately after preparation and enclosed in tubular holders of the same caliber. Equal quantities of samples were studied.

3. Results and discussion

EPR absorption spectra show lines due to Mn^{2+} paramagnetic species within the whole investigated concentration range. These spectra are typical for Mn^{2+} ions in vitreous systems and mainly consist in absorptions centered at g_{eff} = 4.3 and g_{eff} = 2.0 values. The resolution of the spectra is optimal in the low concentration range. For $0.1 \leq x < 10$ mol % both lines are detectable, the $g \cong 4.3$ one hawing the hyperfine structure (hfs) typical for isolated Mn^{2+} ions, well resolved within $0.1 \leq x < 1$ mol %. For $10 \leq x \leq 50$ mol % only the $g \cong 2.0$ absorption line was detected. This one does not show hfs. The spectral structure evolution when rising concentration may be followed in figure 1 for $70TeO_2 \cdot 25B_2O_2 \cdot 5SrO$ glass matrix and in Fig. 2 for those corresponding to $70TeO_2 \cdot 25B_2O_2 \cdot 5SrF_2$ glass matrix. When Mn^{2+} ions enter the matrix in high symmetric sites they are involved in resonances giving raise to signals at $g \cong 2.0$ values. Site to site fluctuations of the crystal field parameters, inherent to glasses, alter the spectral resolution and the inhomogeneous broadening of the line must be taken into account. There are also distortions of the paramagnetic ion vicinity responsible on the local symmetry lowering. For highly distorted sites, strong crystal field effects change the energetic state of the ion and resonances result in signals having $g_{eff} \cong 4.3$ values. The distribution on highly symmetric sites and low symmetric ones of Mn^{2+} ions in the vitreous matrix, may be also followed in the concentration dependence of the EPR absorption spectra by observing the relative intensities of the corresponding signals and their structure.
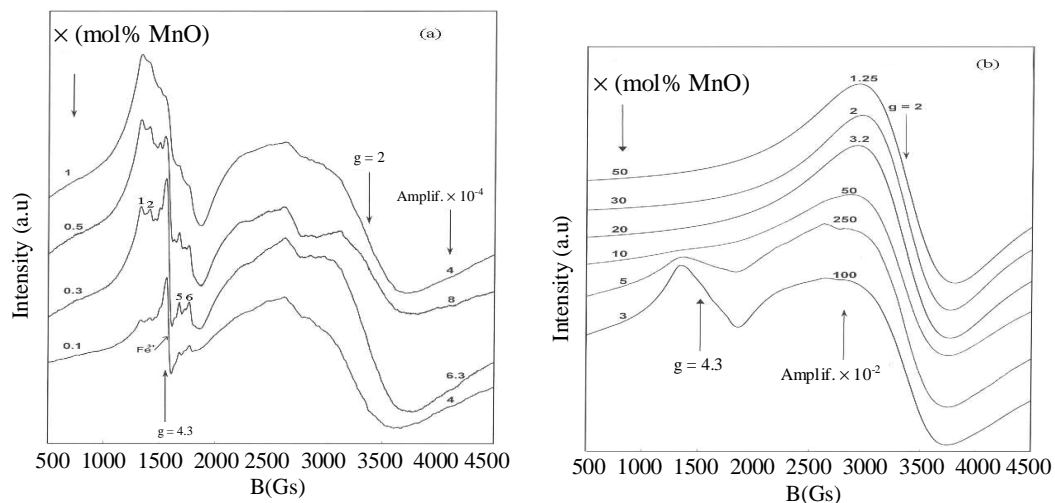

Fig. 1. EPR absorption spectra of Mn^{2+} ions in the $xMnO \cdot (100-x)[70TeO_2 \cdot 25B_2O_3 \cdot 5SrO]$ glasses.

In binary borate glasses previously studied [1-3, 7-12] the lines at $g_{eff} \cong 2.0$ having a well resolved hfs prevail in the spectra, the $g_{eff} \cong 4.3$ ones being much less intense and not resolved. In these glasses B$_2$O$_3$ was the glass former, so the resulted matrix structure allow to Mn^{2+} ions to enter mostly in highly symmetric sites. In our actually studied glass matrices TeO$_2$ as glass former imposes a much more compacte structure. Consequently, the paramagnetic ion structurates its vicinity in a restraint space subjected to closer impact with the neighbouring ions. As isolated ions ordering their vicinity in regular configuration Mn^{2+} impurities were detected only in distorted sites subjected to high crystal field effects, giving rise to the $g_{eff} \cong 4.3$ absorption lines on a relatively short range of concentration (Figs. 1 and 2). These sites are ordered well enough to allow the hfs good resolution. Large distributions of the crystal field parameters even accentuated as rising concentration alter the resolution due to inhomogeneous broadening of the line and the hfs vanishes. Less ordered configurations of Mn^{2+} ion vicinity characterize the sites giving rise to the $g_{eff} \cong 2.0$ absorption lines. The disorder even more increases as raising the MnO content of the matrix so the line symmetrizes along the high concentrations range.
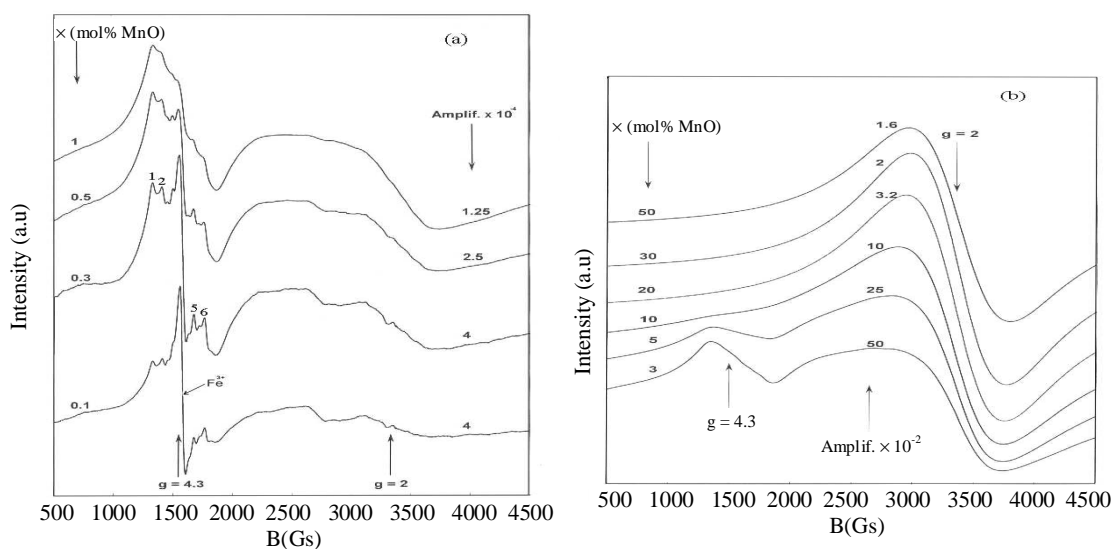

Fig. 2. EPR absorption spectra of Mn^{2+} in the xMnO·(100-x)[70TeO$_2$·25B$_2$O$_3$·5SrF$_2$] glasses.

The paramagnetic impurities distribution on the revealed two types of structural units so as its evolution within the investigated concentration range is almost the same for these two glass matrices (Fig. 1).The third component (SrO or SrF$_2$) do not play a significant part in the matrix structure, from the point of view of the paramagnetic ion energetic state. Only the valence state of impurities seems to be affected during melting when samples were obtained. The Mn^{2+} ions concentration decreased when using SrF$_2$ instead of SrO as third component, fact evidenced by the slight diminution of the $g_{eff} \cong 2.0$ signal intensity for $x \leq 30$ mol%. For $x > 30$ mol% the signal intensity increases in the case of matrix containing SrF$_2$ which is determined by increasing of Mn^{2+} ions in this concentration range [Fig. 3]. Another effect of changing composition might be the lowering of the covalent character of bonds when passing from 70TeO$_2$·25B$_2$O$_3$·5SrO to 70TeO$_2$·25B$_2$O$_2$·5SrF$_2$ glass matrix. This may be observed by comparing the separations between the lines of the hyperfine sextet corresponding to the $g_{eff} \cong 4.3$ signals (Table 1).

Table 1. Composition dependence of the hyperfine separations of the $g_{eff} \cong 4.3$ absorption line.

Glass matrix	x [mol % MnO]	$\Delta B_{1 \leftrightarrow 2}$ [Gs]	$\Delta B_{5 \leftrightarrow 6}$ [Gs]
$70TeO_2 \cdot 25B_2O_2 \cdot 5SrO$	0.1	76.21	91.84
	0.3	74.26	87.93
$70TeO_2 \cdot 25B_2O_2 \cdot 5SrF_2$	0.1	82.07	109.43
	0.3	78.16	91.84
	0.5	72.30	87.93

Because accidental Fe^{3+} ions impurities giving also rise to $g \cong 4.3$ signals the estimation of hf lines separation was done only for the first two and the last two lines of the sextet, to avoid the signal superpositions due to Mn^{2+} and Fe^{3+} lines contribution. According to experimental estimations data in Table 1 the hfs separations are shorter for the $70TeO_2 \cdot 25B_2O_2 \cdot 5SrO$ glasses compared to those corresponding to the $70TeO_2 \cdot 25B_2O_2 \cdot 5SrF_2$ ones for samples with the same MnO content. This involves lower hyperfine coupling of the electronic spin with the nuclear one, that is larger degree of delocalization and consequently, stronger covalent bonding with the ligand ions of the matrix. The hyperfine separation for lines corresponding to the same matrix composition apparently decreases when increasing the MnO content due to the broadening of the individual components of the sextet.
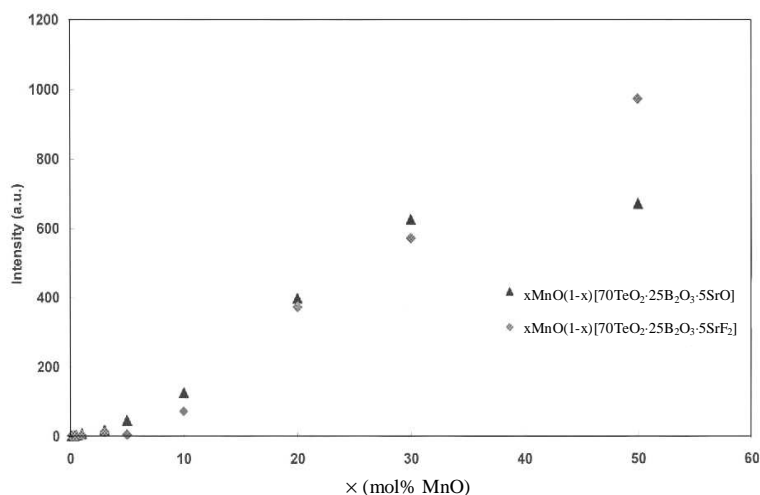
Fig. 3. Composition dependence of the line-intensity of the $g_{eff} \cong 2.0$ EPR signals.

The width of signals at $g_{eff} \cong 2.0$ also depends on concentration, showing an abrupt decreasing up to 10 mol % MnO lowered for $10 < x < 30$ mol % and stopped thereafter (Fig. 4). This evolution reveals clusterizing processes of impurities in both the investigated glass matrices, the line narrowing being determined by the superexchange interactions involving the manganese ions. The line-width values are smaller for signals corresponding to $70TeO_2 \cdot 25B_2O_3 \cdot 5SrF_2$ than those corresponding to the $70TeO_2 \cdot 25B_2O_3 \cdot 5SrO$ glass matrices. By changing SrO with $\cdot SrF_2$ the magnetic coupling between the impurity ions seems to become stronger and to accentuate the exchange interaction.
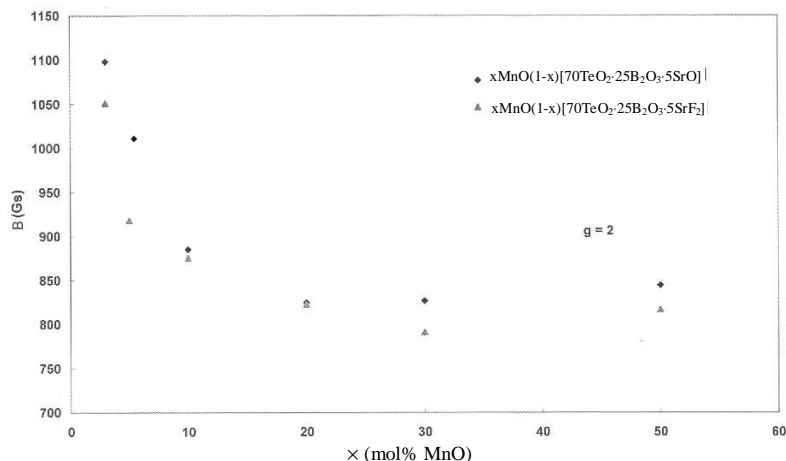
Fig. 4. Composition dependence of the line-width of the g$_{eff}$ $\cong$ 2.0 EPR signals.

4. Conclusions

The EPR investigation of Mn^{2+} ions in the 70TeO$_2$·25B$_2$O$_3$·5SrO and 70TeO$_2$·25B$_2$O$_3$·5SrF$_2$ glass matrices revealed some influences of the matrix composition on the impurities distribution and interactions involving them. The distribution of Mn^{2+} ions on different types of structural units depends on the MnO content. In both systems, up to 5 mol % MnO there are isolated ions in well structurated vicinities, giving rise to absorptions at g$_{eff}$ $\cong$ 4.3 and ions in less ordered vicinities, having tendencies of associate in cluster formations, which give rise to absorptions centered at g$_{eff}$ $\cong$ 2.0 values. The high degree of ordering in the Mn^{2+} ions neighbourhood is attested by the good resolution of the hfs at g$_{eff}$ $\cong$ 4.3 signal. Changes in the matrix composition did not affect spectacularly the spectral structure and its evolution for these signals. There are differences in the hf splitting of the absorption line resulting in shorter separations of the hfs sextet for samples containing SrF$_2$ than those corresponding to SrO containing glasses. This shows less covalent bondings for Mn^{2+} in 70TeO$_2$·25B$_2$O$_2$·5SrF$_2$ glass matrix than in those of the 70TeO$_2$·25B$_2$O$_2$·5SrO glass matrix. Differences were also observed for the g$_{eff}$ $\cong$ 2.0 signals corresponding to ions in disordered vicinities, especially in the absorption line intensity, suggesting a slight decreasing of Mn^{2+} ions concentration when replacing SrO with SrF$_2$, for $5 \leq x \leq 30$ mol %, but for x > 30 mol % these ions content overpass that corresponding the matrix with SrF$_2$. Another effect of changing composition of the vitreous matrix was to accentuate the clusterizing tendencies of Mn^{2+} ions when increasing MnO concentration in the SrF$_2$ containing glasses, attested by a more pronounced narrowing of the line at g$_{eff}$ $\cong$ 2.0 suggesting also a stronger magnetic coupling of the involved ions.

References

[1] A. W. De Wijn, R. F. Van Balderen, J. Chem. Phys. **46**, 4 (1967).
[2] D. L. Griscom, R. E. Griscom, J. Chem. Phys. **47**, 2711 (1967).
[3] P. C. Taylor, P. J. Bray, J. Phys. Chem. Solids **33**, 43 (1972).
[4] D. Loveridge, S. Parke, Phys. Chem. Glasses **12**, 19 (1971).
[5] V. Cerny, B. Petrova, M. Frumar, J. Non-Cryst. Solids **125**, 17 (1990).
[6] V. Cerny, B. Frumarova, J. Rosa, J. L. Licholit, M. Frumar, J. Non-Cryst.Solids **192&193**, 165 (1995).
[7] I. Ardelean, Gh. Ilonca, M. Peteanu, Solid State Commun. **52**(2), 147 (1984).
[8] M. Peteanu, I. Ardelean, V. Simon, S. Filip, M. Flora, Studia Univ. Babes-Bolyai, Physica XLI (2), 11 (1996).
[9] I. Ardelean, M. Peteanu, V. Simon, S. Filip, M. Flora, S. Simon, J. Mater. Sci. **34**, 6063 (1999).

[10] I. Ardelean, M. Peteanu, V. Simon, S. Simon, M. Flora, Phys. Chem. Glasses **41**(3), 153 (2000).
[11] I. Ardelean, M. Peteanu, R. Ciceo-Lucăcel, P. Pascuta, M. Flora, Studia Univ. Babes-Bolyai, Physica XLVI (2), 19 (2001).
[12] I. Ardelean, M. Flora, J. Mat. Sci.: Mat. in Electronics **13**, 357 (2002).
[13] I. Ardelean, Gh. Ilonca, M. Peteanu, D. Pop, Solid State Commun. **33**, 653 (1989).
[14] M. Peteanu, I. Ardelean, S. Filip, D. Alexandru, Rom. J. Phys. **41**(7/8), 593 (1996).
[15] H. H. Wickman, P. H. Klein, D. A. Shirley, J. Chem. Phys. **42**, 2113 (1965).
[16] J. W. H. Schreurs, J. Chem. Phys. **62**, 2151 (1968).
[17] R. C. Niklin, C. P. Poole, H. A. Farach, J. Chem. Phys. **68**, 2579 (1973).
[18] I. V. Chepeleva, E. A. Zhilinskaia, V. N. Lazukin, A. P. Cernov, I. Olkhovskii, Phys. Stat. Sol. B **82**, 189 (1977).
[19] D. W. Moon, J. M. Aitken, R. K. MacCrone, G. S. Cieloszky, Phys. Chem. Glasses **16**, 91 (1975).
[20] R. W. Kedzie, D. H. Lyons, M. Kestigian, Phys. Rev. A, **138**, 918 (1965).
[21] I. V. Chepeleva, DAN SSSR **202**, 1042 (1972).
[22] I. Ardelean, S Filip, J. Optoelectron. Adv. Mater. **5**(1), 157 (2003).